



# INSIGHT GUARD: PIONEERING EARLY GLAUCOMA DETECTION USING MACHINE LEARNING

<sup>1</sup>Saberi Younus Mushtaq, <sup>2</sup>Nanda Kumar V, <sup>3</sup>Nischith PM, <sup>4</sup>Neelesh S, <sup>5</sup>Prof. Priyanka Nilesh Chavan

<sup>1,2,3,4</sup>Student, Department of Computer Science and Engineering, AMC Engineering College, Bengaluru, Karnataka, India.

<sup>5</sup>Professor, Department of Computer Science and Engineering, AMC Engineering College, Bengaluru, Karnataka, India.

**Abstract:** A Chronic eye disorder called glaucoma leading to irreversible blindness by damaging the optic nerve of the eye. It is provoked due to exalted intraocular pressure inside the eye. Detecting glaucoma is the most challenging process in case of open angle glaucoma (OAG) due to lack of initial symptoms. Detecting glaucoma in the early stage is required to facilitate appropriate monitoring, treatment, and to diminish the likelihood of vision loss. In this paper, we propose a method to analyse and categorize the fundus image as glaucomatous or healthy image by employing image processing techniques to take into account the cup to disc ratio and feature extracted through Deep learning. The first step in identifying glaucoma is to measure CDR, which rises from 0.6 to 0.9 in cases of the condition. The Deep Learning-Convolution neural network model is used to automate the glaucoma diagnostic procedure and take into account additional medical data. Overfitting is avoided by adopting data augmentation technique. To make the system user friendly and interactive Graphical user interface (GUI) application is developed. The system is trained, and the outcomes show that the method performed well in categorizing the fundus images as healthy or glaucoma.

**Index Terms** - Glaucoma, Fundus images, Open angle glaucoma (OAG), Cup to disc ratio (CDR), Graphical User Interface (GUI), convolutional neural networks, and deep learning methods.

## I. INTRODUCTION

Vision is essential in everyone's life to visualize the things around us but there is vision loss in many people due to few eye related diseases. According to 2019 survey of World Health Organization, 2.2 billion people are suffering from several eye related diseases among which 39 million people are completely blind. The overall percentage of the eye diseases which causes blindness are 47.8% is due to cataract, 12.3% for glaucoma, 8.7% for age related macular degeneration, 4.8% of diabetic retinopathy, 5.1% due to corneal opacities. Major challenging task is to detect glaucoma in the early stages which is the second main cause for the vision loss worldwide. Glaucoma is a chronic disease which develops and progresses slowly and finally leads to blindness if not treated early. Thus, the term "silent thief of vision" applies. Glaucoma patients cannot recognize the vision impairment during the initial days, later the disease progresses gradually leading to complete vision loss. Optic nerve deterioration takes place due to glaucoma.

Glaucoma symptoms are painless and leads to vision loss in the final stages. Hence, early detection is required in order to prevent the vision loss. Eye consists of two types of fluids namely vitreous humor and aqueous humor. Aqueous humor has a stable intra ocular pressure (IOP) of 21 mmHg and to maintain stable IOP, aqueous humor is periodically secreted and drained out. Sudden increase in the IOP takes place due to blockage of channels where aqueous humor is not drained out. Now, the pressure inside the eye will be more than 21 mmHg which leads to more pressure on the optic nerve fibers. Nerve fibers gets damaged due to the elevation in the IOP causing glaucoma disease. Due to glaucoma, blood vessels get flattened and cup area of the optic nerve increases with constant optic disc area so that cup to disc ratio (CDR) enhances. This disease can also occur due to poor blood regulation to the optic nerve in the presence of normal eye pressure.

Glaucoma is associated with vision impairment due to the damage of the optic nerve fibers, therefore it is termed as optic nerve disease, where optic nerve acts as a mediator between the eye and brain to visualize by sending and receiving the message signals. So, if optic nerve gets damaged then brain cannot receive and send signals to eye and vice versa. The two types of Glaucoma are open angle and closed angle (angle closure) glaucoma. Open angle glaucoma is painless and has no symptoms and develops progressively. Vision loss can be prevented by detecting glaucoma in the early stages. Currently, OCT (Optical coherence Technique) and HRT (Heidelberg retinal Tomography) are the techniques used for the detection of glaucoma. OCT scanning is the currently used technique for detecting glaucoma depending on energy levels. In OCT scanning low coherence light is utilized for imaging of cross-sectional view of the retina. Images obtained from the OCT scanning may be two or three dimensional. HRT is a technique used to capture the optic nerve by using lasers to get three dimensional images. This technique makes use of inner layers of the retina that forms the optic nerve, when person is affected by glaucoma, cells forming optic nerve fibers gets damaged due to which the region where optic nerve get damaged, optical cupping will occur. The depth of the cupping is examined by the ophthalmologist to detect glaucoma. But two techniques used are prolonged and expensive. So, many ophthalmologists use fundus images for diagnosis of glaucoma. Fundus images are captured using fundus camera. Fundus images are the two-dimensional images of the retina. Fundus images contains macula at the center and optic disc either on the left or right side depending on left eye or right eye. The color of these images is orange color due to the presence of rhodopsin pigment and complexes of vitamin B12 and intensity of this color gets diminished as the age of person increases. Healthy and glaucoma image are shown in Figure 1 and Figure 2 respectively.



**Figure 1:** Healthy Fundus Image



**Figure 2:** Glaucoma Image

## II. LITERATURE SURVEY

Lauren Coan, Bryan Williams, et al.,[1] have provided a comprehensive review of the current state-of-art of artificial intelligence-enabled glaucoma detection frameworks that produce and use segmented fundus images. They have identified two main approaches: logical rule-based frameworks and machine learning/statistical modelling frameworks and summarised the advantages and limitations of each approach, as well as the key challenges and opportunities for future research. The proposed idea for AI framework for glaucoma detection should be able to provide accurate, interpretable, and explainable results, while also being generalisable, scalable, and clinically relevant. It suggests that combining clinically interpretable features with

abstract features, and using ensemble or hybrid classifiers, could improve the performance and robustness of the AI frameworks. It also recommends that more external validation, standardisation, and reporting of the AI methods are needed to ensure their reliability and applicability in real-world settings. However, it has been acknowledged that there are some drawbacks and limitations. First, it only focused on fundus imaging as the modality for glaucoma detection, while other modalities such as OCT or visual field tests could also provide valuable information. Second, it only considered AI frameworks that produce and use segmented fundus images, while some recent studies have shown that end-to-end image classification methods using deep learning can achieve comparable or superior results without segmentation. Third, it did not perform a meta-analysis or a systematic comparison of the AI frameworks, due to the heterogeneity and variability of the data sources, methods, and metrics used in the literature.

P.M. Siva Raja, S. L. Jothilakshmi et al.,[2] have presented a comprehensive review of deep learning algorithms and their applications for glaucoma detection from various types of medical images. It has summarized the main concepts, advantages, and challenges of different deep learning architectures, such as convolutional neural networks, autoencoders, deep belief networks, and restricted Boltzmann machines<sup>1</sup>. It has also surveyed the use of deep learning for various tasks related to glaucoma diagnosis, such as optic disc and cup segmentation, retinal nerve fiber layer defect detection, cup to disc ratio estimation, and glaucoma screening and classification. The proposed idea is to provide a useful reference for researchers and practitioners who are interested in applying deep learning techniques for glaucoma detection and to highlight the potential and challenges of this emerging field. This approach also included some drawbacks that it is not very systematic and comprehensive, as it does not follow a clear and consistent methodology for selecting, analysing, and synthesizing the relevant literature. It does not provide clear inclusion and exclusion criteria, quality assessment, or meta-analysis of the studies they review.

Pooja Sharma et al.,[3] have reviewed the current literature, on diagnostic tools for glaucoma detection and management, with an emphasis on the best evidence available to support their use in clinical practice. They have discussed the advantages and limitations of various techniques for assessing structural and functional damage in glaucoma, such as optic disk photography, confocal scanning laser ophthalmoscopy, scanning laser polarimetry, optical coherence tomography, standard automated perimetry, short-wavelength automated perimetry, and frequency-doubling technology perimetry. However, it has been acknowledged that there are some drawbacks and challenges in the use of diagnostic tools for glaucoma. These include the variability and reproducibility of the measurements, the influence of ocular and systemic factors on the test results, the lack of standardized criteria and methods for defining and detecting glaucoma and its progression, and the need for further validation and comparison studies in large and diverse populations. They also emphasize that the diagnosis and management of glaucoma should not rely solely on the results of imaging and perimetry devices, but should also incorporate other relevant parameters, such as intraocular pressure, optic nerve head appearance, patient history, and risk factors.

Amed Mvoulana, Rostom Kachouri, et al.,[4] proposed a new fully automated method for glaucoma screening and diagnosis from retinal fundus images. Their method consists of four stages: optic disc detection, optic cup and optic disc segmentation, cup-to-disc ratio calculation, and glaucoma classification. They evaluated their method on the DRISHTI-GS1 dataset and achieved 98% accuracy, outperforming the state-of-the-art methods based on the cup-to-disc ratio feature. Their method is also computationally efficient and suitable for mobile implementation. However, their method also has some limitations and drawbacks. First, their method relies on the assumption that the optic disc is the brightest region in the image, which may not hold true for some pathological cases or image quality issues. Second, their method uses a fixed threshold to segment the optic cup and optic disc, which may not be optimal for different image characteristics or variations. Third, their method uses only one feature, the cup-to-disc ratio, to classify glaucoma, which may not capture the full complexity and diversity of the disease. Fourth, their method was tested on a relatively small and homogeneous dataset, which may limit its generalizability and robustness to other populations and settings.



Natalie Schellack, Gustav Schellack, et al.,[5] have provided a brief, synoptic overview of glaucoma, a complex condition of the eye that is the second leading cause of blindness worldwide. They have discussed the pathophysiology, classification, signs, symptoms, diagnosis, risk factors, and pharmacological treatment options of glaucoma. They have also highlighted some of the challenges and limitations of the current therapies, such as poor patient adherence, adverse effects, drug interactions, and inadequate IOP control. The proposed idea that the future research should focus on developing better therapeutic options that can address the underlying mechanisms of glaucomatous optic neuropathy, prevent or reverse retinal ganglion cell death, and preserve visual function. They also suggest that novel drug delivery systems, such as nanotechnology, gene therapy, and stem cell therapy, may offer promising avenues for improving the efficacy, safety, and convenience of glaucoma treatment. However, they acknowledge that these approaches are still in their infancy and face many technical, ethical, and regulatory hurdles before they can be translated into clinical practice. Therefore, they conclude that glaucoma remains a major public health challenge that requires continuous efforts from researchers, clinicians, and patients to prevent vision loss and improve quality of life.

Alessandro A Jammal, et al.,[6] propose a novel machine-to-machine (M2M) deep learning (DL) algorithm that can quantify glaucomatous damage on fundus photographs by predicting retinal nerve fiber layer (RNFL) thickness from spectral-domain optical coherence tomography (SD OCT). They compare the performance of the M2M DL algorithm with that of human graders in detecting eyes with glaucomatous visual field loss. They show that the M2M DL algorithm has a stronger correlation with visual field metrics and a higher diagnostic accuracy in the region of high specificity than human graders. The M2M DL algorithm has several advantages over previous DL models trained based on subjective human gradings. It provides objective and quantitative assessment of neural damage, avoids the biases and errors of human graders, and can be easily adjusted according to the desired level of specificity and disease stage. However, the M2M DL algorithm also has many shortcomings that should be addressed in upcoming research. For example, the algorithm may not capture subtle sectoral RNFL losses, as it was trained with a global RNFL parameter. Moreover, the algorithm needs to be validated in external data sets and different populations, as well as refined to detect localized RNFL or rim loss. Finally, the algorithm requires high-quality fundus photographs and SD OCT scans, which may not be available in all settings.

Hina Raja et al.,[7] presented a novel method for detecting glaucoma, computing cup to disc ratio by using OCT scanned images i.e. spectral domain (SD OCT) images. Optic cup diameter is extracted using the inner limiting membrane (ILM) and optic disc diameter has been obtained using Retinal Pigment Epithelium (RPE). The two layers of the SD OCT images are ILM and RPE. Initially the region containing cup i.e. ILM layer is separated earlier to extraction of the Retinal Pigment Epithelium layer to calculate diameter of the cup. Since green channel is more prominent with cup and disc region. Further green channel is used for extraction of cup and disc diameter. First, cup diameter is computed depending on the threshold value then after disc diameter is calculated by removing ILM layer, afterwards applying threshold for 5- levels then RPE layer is extracted after processing RPE layer for calculation of disc diameter. After calculating cup and disc diameter, CDR is evaluated for the computed cup and disc diameter.

U. Raghavendra et al.,[8] has propounded a different method of detecting glaucoma using deep convolutional neural networks. This is a novel method of recognition of glaucoma using CAD (Computer Aided diagnosis) which is a non-intrusive technique for identification of glaucoma in the initial stages using digital fundus images. This system is developed using large dataset to get more accurate and efficient results by using CAD tool to implement deep learning technique. Using deep learning, 18 layers of convolutional neural networks, fundus images are classified as glaucomatous or healthy by extracting the features required. By training the model robustly, they are achieving the more accuracy and increase in the performance factor.

### III. PROPOSED METHOD

In this paper, detection of glaucoma in the initial stages in order to prevent vision loss by estimating cup to disc ratio using image processing. Further to automate the disease detection process deep learning algorithms are implemented. CDR value is determined after separating optic disc and cup employing image processing

techniques. By using image processing the segmentation will be easier. Image processing is rapid, requires less time, advantageous and it will give fruitful results and more profitable. It does not require any chemicals to capture the images and increases the quality and removes the noise in the image required for the diagnosis of the disease. Some of the main features of the medical images requires edges which are preserved and can be used for collecting information for the medical analysis. We can get each and every pixel in the image that is needed for our analysis process. Hence, digital image processing techniques are used for our disease detection process.

Further to automate the disease detection procedure machine learning can be used. Machine learning is the process of training the model with datasets and model learns by itself during the training process and able to classify the given images as glaucoma and healthy images. Machine learning needs to extract the features manually then classification is done by the system considering the features extracted. But extracting features from the fundus image is more complex and are sensitive. DL algorithms extract more features and then divide them as healthy and glaucomatous. Deep learning is training the model using more datasets. Since, feature extraction and classification will be done by the model itself exactly by using the training data. Convolutional neural networks are used for the extraction and classification purpose.

Glaucoma is such a chronic disease need to be detected in its earlier stages using computed CDR value. The constraint in the recognition process of glaucoma is CDR value. To calculate CDR, image processing techniques are employed and further, automate the detection process by applying it to a Deep learning model in order to include more features for classification because, the glaucoma can also be detected using other parameters to get more accurate results. After detecting whether the person is affected by glaucoma or not is pinged through mobile to patients and ophthalmologist for further treatment. Flow diagram of proposed method is illustrated in Figure 3.

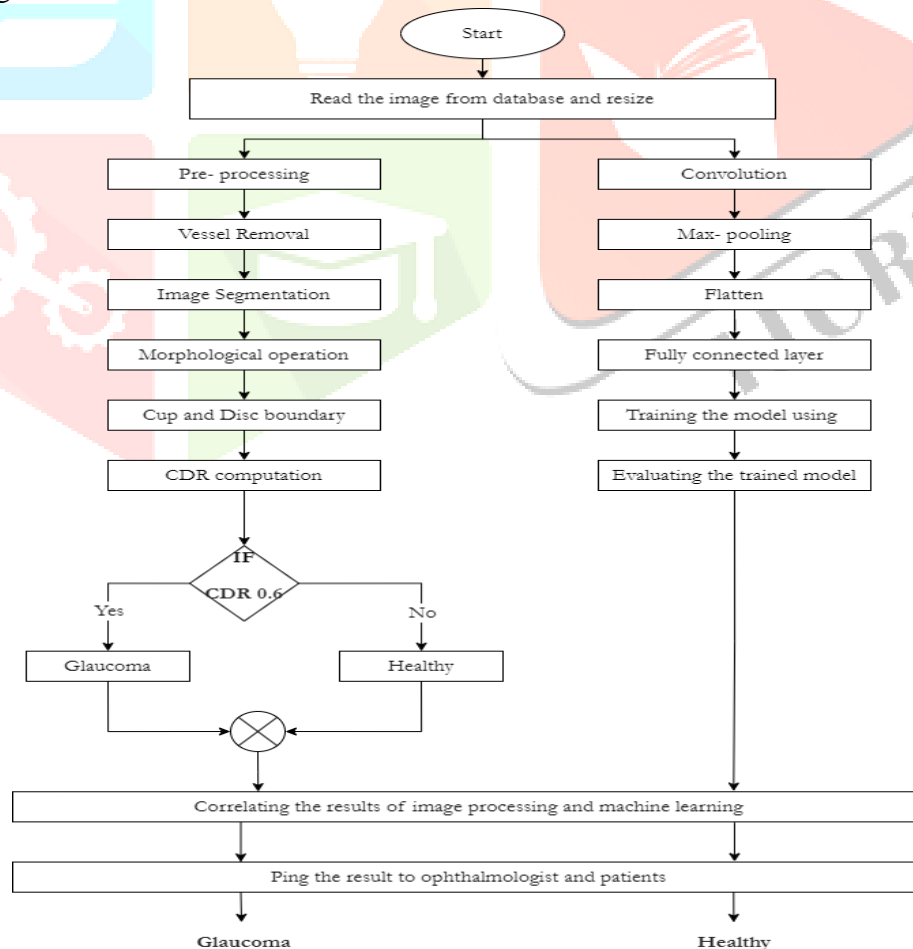


**Figure 3:** Flow Diagram of proposed method

### 3.1 Using Image Processing

To determine glaucoma calculation of CDR value is required. CDR is evaluated by extracting the disc and cup regions using image processing techniques. Retinal fundus image is obtained from fundus camera

which captures the illumination reflected from the retinal surface. The dataset includes 30 fundus photos, 15 photographs of healthy eyes, and 15 images with open angle glaucoma from individuals aged 20 to 70. Images acquired are pre-processed in order to enhance the performance of the image processing like Image transform, Segmentation, Feature extraction etc. and also to remove the noise which may cause problems while disease detection. Pre-processing contains resizing the images, image normalization, removal of noise.

### 3.2 Optic Disc Extraction

The higher intensity or the brightest region of the fundus image is optic disc, where rods and cones are not present often known as blind spot. The beginning of the optic nerve is optic disc. An algorithm is proposed to detect optic disc.

Retinal fundus Image from the dataset is read as input randomly. Initially, images are resized to 240 x 240 required for further processing. Region of interest (ROI) is extracted prior to the pre-processing of the fundus images. ROI is the region contains the information required for the detection process. The reason behind the extraction of region of interest is to reduce the image size and also to reduce the complexity of the further tasks which are performed for detection process. The first step in the partitioning of optic disc is to extract the ROI as shown in Fig 4. To expedite the CDR computation and ensure precise extraction of the ROI region. ROI will be less than 11% of the Fundus image. By observation we can say that optic disc region contains more brighter pixels in comparison with the other pixels of the image. Pixels at the optic disc center has highest intensity. Boundary of ROI is double the diameter of the optic disc, used to segment optic disc and cup. By extracting the region of interest, it is easy to segment required region.

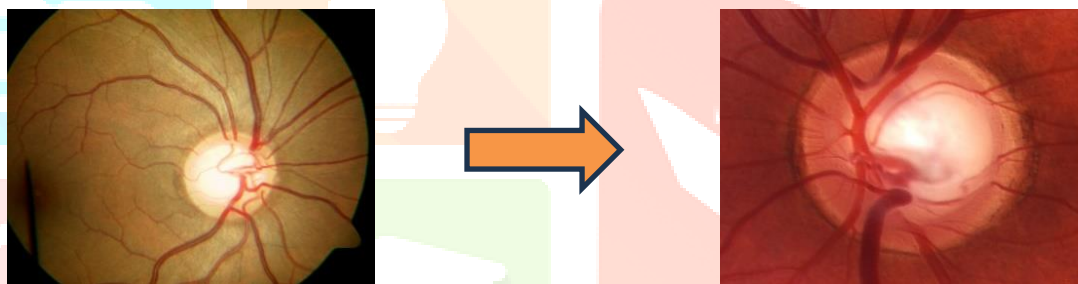


**Figure 4:** ROI extracted

BGR system of colors used for computer display. BGR images are converted to grayscale as grayscale images are easier for further processing because grayscale images contain only the darkest shade is black and the lightest shade is white. Since grayscale contains only two colors black and white it is easy to detect the higher intensity and lower intensity pixels easily. Gray image is fed as input to the gaussian filter. Gaussian blur is a linear filter, which is also called as gaussian smoothing, which performs the blurring operation so that noise can be reduced. Image blurring will be done by Gaussian function as shown below.

$$G(x, y) = \frac{1}{2\pi\sigma^2} e^{-\frac{x^2+y^2}{2\sigma^2}}$$

where, x and y are the horizontal and vertical distance from origin respectively and  $\sigma$  is the standard deviation of the gaussian function. To find the max location Minmax function is used, which outputs the minimum and maximum intensities of the image along with the location of the minimum and maximum intensities. The computation of finding maximum intensities is carried on by finding out one highest intensity pixel later by updating each pixel by comparing with the neighbouring pixels in the ROI. By observation we know that higher intensity is nearer to the optic disc and cup. So, by localizing the higher intensity pixels along with the position of the pixels and then shape fitting on the optic disc.

### 3.3 Optic Cup Extraction

Optic disc has white cup like area called optic cup. Fig 7 illustrates the optic cup extraction. RGB image is read and then region of interest is cropped as per the concept of max intensity location. To segment the cup

region inside optic disc (OD), Pixels of the green channel are more prominent since they have more contrast, visibility and brightness.

Image is split into R, G, B channels. Closing operation is performed in order to fill the boundary pixels of image by applying dilation followed by erosion. Enhancing the contrast of the fundus image using stretching operation, by replacing the certain intensity pixel values to a preferred intensity value. Initially if any image has to be normalized, we have to specify the lower and higher pixels values. These limits will act as minimum and maximum pixel values. The limits can be calculated using the below equation.

$$P_{out} = (P_{in} - c) \left( \frac{b-a}{d-c} \right) + a$$

If the values are less than 0 are replaced by 0 and greater than 255 are replaced by 255. Mainly contrast stretching is applied to visualize the optic cup prominently. In RGB, separation of color information from luminance is not possible. Hence using HSV we can separate image color information from luminance. 'Hue' represents color, 'saturation' represents how much of amount of color is added is with white, 'value' represents how much of amount of color is added with black. Median filtering is applied on the saturation channel which removes the noise where Optic cup region is more prominent in S channel. Median filter replaces all the pixels by the median value calculated for further cup extraction. Color enhancement is done in order to improve the contrast for better segmentation of cup region. LAB color space is formed by converting HSV image to enhance the color space of the cup region for segmentation.

An unsupervised iterative technique called k-means clustering, has n number of observations are classified as k number of clusters. Centers for k clusters are chosen randomly. Allocating each pixel to the cluster as it reduces the distance from the centers. For the reduction of noise in the clusters by applying it to a bilateral filtering to preserve edges. Canny Edge Detector is used to apply noise suppression to the bilateral filtered picture in order to detect the edges of the optic cup. Contour is used for combining all the points along the boundary containing same intensity pixels for object detection and analysing the shape of the object. Boundaries are smoothed using linear ellipse fitting, after extracting the edges. To fit an ellipse Least square fitting algorithm is used which smoothens the edges after detecting edges using canny edge detectors. After fitting an ellipse to the optic cup, optic cup will be extracted.

#### IV. CLINICAL TERMINOLOGY AND BRIEF BACKGROUND

##### 4.1 Cup to disc ratio

The cup-to-disc ratio (CDR) is a widely accepted metric to characterize glaucomatous neuropathy, obtained from assessment of the ONH. There are different variants of the CDR parameter. The area cup-to-disc ratio (ACDR) and the vertical cup-to-disc ratio (vCDR) are the two main ones, though.

The vCDR is defined as:

$$vCDR = \frac{\text{Vertical Cup Diameter}}{\text{Vertical Disc Diameter}}$$

The ACDR is defined as:

$$ACDR = \frac{\text{Area of Cup}}{\text{Area of Disc}}$$

Despite being widely utilized in practice, the CDR parameter is constrained in big OC cases, genetically large or small OD cases, and cases where myopic ONH alterations are present. In these situations, the CDR can be deceptive and result in diagnostic errors. Additional morphometric characteristics, like the rim-to-disc ratio (RDR) and horizontal cup-to-disc ratio (hCDR) can also be considered. A reduction in the RDR, as opposed to the CDR, signifies glaucomatous neuropathy. The ACDR offers a feature-based, two-dimensional assessment that permits structural changes of the ONH to be assessed.

##### 4.2 Neuroretinal rim area ratio

The Neuroretinal Rim (NRR) is the area between the OC margin and the OD margin which comprises retinal nerve fibre axons. The region that remains after deducting the OC from the OD in fundus pictures is called the NRR. The nasal, temporal, superior, and inferior quadrants make up the NRR.



The NRR area is calculated as:

$$NRR = \frac{\text{Area in Inferior Quadrant} + \text{Area in Superior Quadrant}}{\text{Area in Nasal Quadrant} + \text{Area in Temporal Quadrant}}$$

As a general rule, the four NRR quadrants should meet the inferior-superior-nasal-temporal (ISNT) rule (I>S>N>T). The ISNT rule concentrates on the NRR width, or the space between the OC and OD boundaries, whereas the cup-to-disc ratio parameter concentrates on the OC size in relation to the OD. In a healthy eye, the nasal rim is thicker than the temporal rim, and the inferior rim is thicker than the superior rim, according to the ISNT rule. Any infraction of the ISNT rule may be interpreted as evidence of glaucomatous neuropathy. This isn't always the case, though; a robust NRR may nevertheless defy the regulation. Because of this, the ISNT rule is regarded as a therapeutic aid rather than a diagnostic exam.

## V. ALGORITHM AND FRAMEWORKS USED

### 5.1 Convolutional Neural Networks (CNN):

CNNs, or convolutional neural networks, are a subclass of deep neural networks created especially for processing structured grid data, such as images. They consist of multiple layers, including convolutional, pooling, and fully connected layers, enabling them to automatically learn hierarchical representations of data. The fundamental operation in a CNN is the convolution operation, defined as follows:

$$S(i,j) = (I * K)(i,j) = \sum_m \sum_n I(m,n) \cdot K(i - m, j - n)$$

Here, I is the input image, K is the convolutional kernel, and S is the feature map. The kernel is convolved with the input image, producing the feature map that captures local patterns. Pooling layers, often used after convolutional layers, reduce the spatial dimensions of the input, reducing computation while preserving important features. A common pooling operation is max pooling, defined as:

$$P(i,j) = \max_{m,n} I(2i + m, 2j + n)$$

Fully connected layers connect every neuron from one layer to every neuron in the next, providing high-level representations. The output of a fully connected layer is given by:

$$y_k = \sigma \left( \sum_i w_{ki} x_i + b_k \right)$$

Here,  $w_{ki}$  represents the weight connecting neuron i to k,  $x_i$  is the input to the layer,  $b_k$  is the bias term, and  $\sigma$  is the activation function.

CNNs excel in image-related tasks due to their ability to capture hierarchical features through learned filters, making them powerful tools for glaucoma detection.

### 5.2 Optic Disc and Cup Segmentation using U-Net:

Convolutional neural network architecture U-Net was created with semantic segmentation tasks in mind. It is particularly effective in segmenting structures like the optic disc and cup in medical images. The U-Net architecture comprises an encoding path and a decoding path. The contracting path captures context through convolutional and pooling layers, while the expansive path enables precise localization using up sampling and convolutional layers.

The loss function used in U-Net for segmentation tasks is often the Dice coefficient, which measures the overlap between predicted and ground truth segmentation masks:

$$DSC = \frac{2 \times |X \cap Y|}{|X| + |Y|}$$

Here, X and Y represent the predicted and ground truth binary masks. The closer the Dice coefficient is to 1, the better the segmentation accuracy. U-Net's skip connections facilitate the direct transfer of low-level features to the expansive path, mitigating the vanishing gradient problem and aiding in accurate segmentation.



### 5.3 VGG19:

VGG19 is a variant of the VGG (Visual Geometry Group) architecture, known for its simplicity and effectiveness. VGG19 has 19 weight layers and is widely used for image classification tasks. The architecture comprises convolutional layers with small receptive fields (3x3), followed by maxpooling layers. The convolutional layers are defined as:

$$F^l_{i,j} = \sigma(\sum_{m,n} W^l_{i,j,m,n} A^{l-1}_{m,n} + B^l_{i,j})$$

Here,  $F_{i,j,l}$  is the activation at position (i,j) in layer l,  $W^l_{i,j,m,n}$  represents the weights,  $A^{l-1}_{m,n}$  is the activation from the previous layer,  $B^l_{i,j}$  is the bias, and  $\sigma$  is the ReLU activation function.

VGG19's architecture facilitates feature learning through stacking convolutional layers, leading to impressive performance in image classification tasks.

In summary, these algorithms play vital roles in glaucoma detection, with CNNs serving as versatile feature extractors, U-Net excelling in semantic segmentation, and VGG19 demonstrating strong capabilities in image classification tasks.

### 5.4 SVM Model:

This consists of the following steps:

- Labelling of data
- Generation of vocabulary
- Creation of document-term matrix

Following the labeled data's conversion into a data matrix using the vocabulary's values, the values are then plotted and optimal hyperplane is chosen based on the convex hull. The optimal hyperplane is chosen in a manner that optimizes the training data margin. After the classifier has been trained, the input data is supplied to it so that it can distinguish between positive and negative bullying occurrences. This input data for testing purposes is also converted into data matrix and this data matrix is passed to the classifier. SVMs use sophisticated statistical learning theory to overcome the curse of dimensionality. To establish similarity between data points, kernel functions can be utilized in place of specifying the feature vector.

## VI. PERFORMANCE ANALYSIS

Using the dataset in this part, the performance analysis of the suggested CNN with the U-Net and DenseNet-201 model is evaluated. Parameters including accuracy, precision, recall, specificity, and F-measure are used to assess the model. Additionally, a comparison analysis is carried out to verify the suggested model. The result is contrasted with other deep learning models that are currently in use for CNN classification, like VGG-19, Inception ResNet, ResNet 152v2, and DenseNet-169. All of the experiments are implemented and run using the Simulink toolbox in MATLAB 2019a. The dataset is split into 75% for training and 30% for validating the performance analysis.

### 6.1 Performance Metrics

The main goal of this study is to identify glaucoma from retinal fundus images, which can be helpful in determining whether or not the patient has glaucoma. Depending on whether the model's output indicates that glaucoma is present or not, the results can be either positive or negative. To estimate the result of this model, the true positive, true negative, false positive, and false negative are appropriately examined.

- TP: it indicates the total predictions correctly obtained in positive cases
- FP: it indicates the total predictions incorrectly obtained in positive cases
- TN: it indicates the total predictions correctly obtained in negative cases
- FN: it indicates the total incorrect predictions in negative cases

Accuracy is the model's estimation of the performance subset. In order to determine how effective the categorization process is, this is the main output statistic. Typically, estimation is done when both the positive and negative classes are equally important. It is calculated using the following equation.

$$\text{Accuracy} = \frac{TP + TN}{TP + TN + FP + FN}$$

Table 1 illustrates how the suggested model performed better in terms of classification accuracy throughout both training and testing for classifying the glaucoma fundus images. Compared to other methods, the model's training accuracy was 98.82%, an improvement of 1.09% to 3.96%. The accuracy of the tests is 96.90%, or 1.36% to 5.26% increased performance than the other existing compared models. The graphical chart of the comparison is plotted in Figure 5.

**Table 1:** Performance analysis of accuracy.

Models	Training	Testing
VGG-19	97.73	95.54
Inception ResNet	94.86	91.64
ResNet 152v2	97.56	93.21
DenseNet169	97.14	95.45
Proposed	98.82	96.90

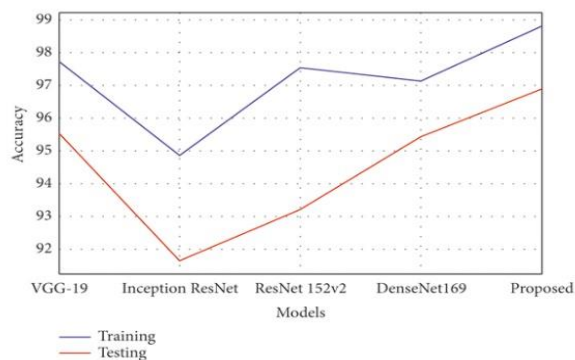


**Figure 5:** Graphical plot of accuracy

Precision is a positive predictive value. It is a measurement of the successfully anticipated positive observation's cumulative predictive positive value. The reduced precision value indicates that the classification model has been impacted by a significant amount of false positives. The following formula can be used to calculate the precision measure.

$$\text{Precision} = \frac{TP}{TP + FP}$$

Table 2 presents the precision estimation results, indicating that the suggested model outperformed the compared models in terms of precision value. In training, the model achieved a precision rate of 98.63%, an improvement of 1.1% to 4.8% over alternative methods. With a precision rate of 96.45% during testing, the model outperformed the other existing comparator models by 1.08% to 4.9%. Figure 6 shows the comparison of precision analysis.

**Table 2:** Performance analysis of precision.

Models	Training	Testing
VGG-19	97.30	94.70
Inception ResNet	93.81	91.52
ResNet 152v2	97.28	93.02
DenseNet169	97.49	95.37
Proposed	98.63	96.45

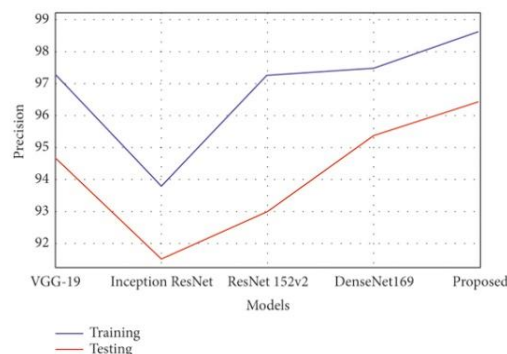


**Figure 6:** Graphical plot of precision

The sensitivity is also referred to as recall. It is the proportion of the total positive predictive value that is correctly anticipated as positive. The reduced recall value indicates that the classification model has been impacted by a significant amount of false negative values. The following formula can be used to get the recall estimation.

$$\text{Recall} = \frac{TP}{TP + FN}$$

As shown in Table 3, the suggested model has improved in terms of recall or sensitivity rate. The model obtained 98.95% recall rate in training, which was 1.1% to 4.05% improved compared with other techniques. In testing, the recall rate was 97.03%, outperforming the other evaluated models by 1.3% to 5.06%. The comparison graph is plotted, as shown in Figure 7.

**Table 3:** Performance analysis of recall.

Models	Training	Testing
VGG-19	97.84	95.62
Inception ResNet	94.90	91.97
ResNet 152v2	97.62	94.05
DenseNet169	97.35	95.69
Proposed	98.95	97.03

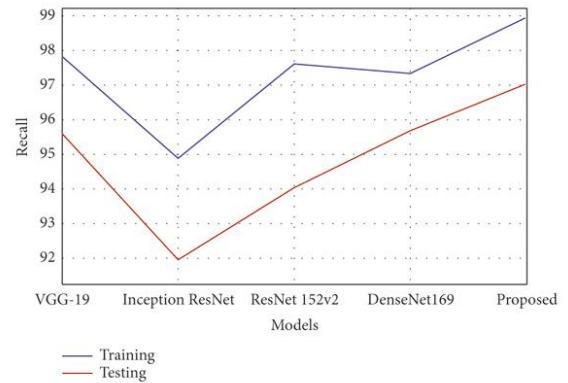


**Figure 7:** Graphical plot of recall

The prediction that healthy patients do not develop the disease is known as specificity in this paradigm. It is the proportion of healthy individuals that test negative. The specificity estimation can be calculated using the following equation.

$$\text{Specificity} = \frac{TN}{TN + FP}$$

The suggested model has a higher specificity rate than the other comparison model, as indicated in Table 4 models of deep learning. In training, the model achieved a 98.15% specificity rate, an improvement of 0.8% to 4.1% over alternative methods. The specificity rate in testing was 96.33%, which was 0.6% to 6.4% better performance than the other existing compared models. Figure 8 represents the comparison of specificity estimated.

**Table 4:** Performance analysis of specificity.

Models	Training	Testing
VGG-19	97.24	95.67
Inception ResNet	94.05	89.92
ResNet 152v2	97.28	92.73
DenseNet169	97.00	94.89
Proposed	98.15	96.33

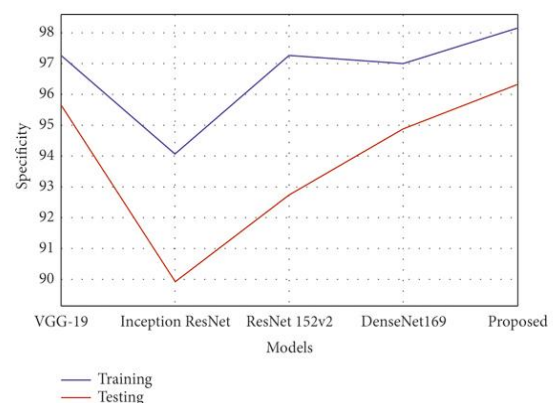


**Figure 8:** Graphical plot of specificity

The weighted harmonic mean of the test's precision and recall is known as the F-measure, and it is used to estimate the test's accuracy. The accuracy does not account for the distribution of the data. The distribution problem is then accurately managed by applying the F-measure. It was helpful when there were unbalance classes in the data set. The following formula can be used to determine the F-measure estimation.

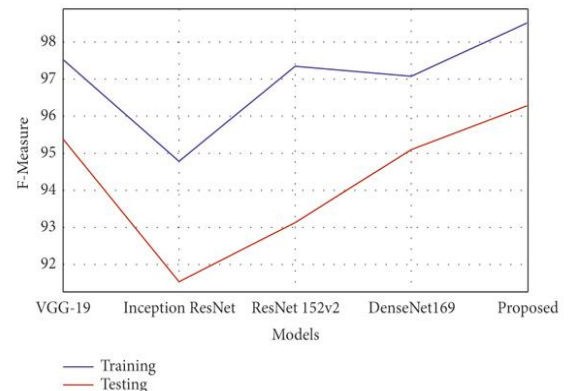
$$F - \text{measure} = \frac{2 \times \text{Precision} \times \text{Recall}}{\text{Precision} + \text{Recall}}$$

Table 5 displays the F-measure estimation, indicating that the suggested model has succeeded in better F-measure value than the compared models. The model obtained 98.50% F-measure rate in training, which was

0.9% to 3.7% improved compared with other techniques. With an F-measure rate of 96.28% throughout testing, this model outperformed the other evaluated models by 0.8% to 4.7%. The contrast of F-measure analysis is displayed in Figure 9.

**Table 5:** Performance analysis of F-measure.

Models	Training	Testing
VGG-19	97.52	95.39
Inception ResNet	94.79	91.55
ResNet 152v2	97.35	93.14
DenseNet169	97.07	95.09
Proposed	98.50	96.28



**Figure 9:** Graphical plot of F-measure

In this study, the suggested model outperformed all other models, including VGG-19, Inception ResNet, ResNet 152v2, and DenseNet-169, in both the training and testing phases. DenseNet-169 performs fairly close to the suggested model, while Inception ResNet achieves the least performance.

## VII. CONCLUSION AND FUTURE WORK

Glaucoma is optic nerve disease caused due the increased intraocular pressure which leads to complete vision loss if it is not detected in the initial stages. Thus, detection of disease in the early stages is necessary. Here we accomplish the detection process in the early stages using image processing techniques considering CDR value and by automating the detection using process using deep learning algorithms by extracting other features of the fundus image and achieved an accuracy of 84.51%. Later, Correlating the results of image processing and deep learning to make the system efficient. This technique gives a best solution compared to the currently existing technologies as they need plenty of time to detect the disease and expensive. This disease detection process will assist the ophthalmologist to treat the glaucoma affected patients more accurately and also results are pinged to patients and ophthalmologist. This disease detection can be extended for other eye related diseases like, Age-related macular degeneration (AMD), diabetic retinopathy etc. Fundus camera can be developed to capture the fundus images.

## REFERENCES

- [1] Lauren Coan, Dr. Bryan, Mr. Krishna, "Automatic Detection of Glaucoma via Fundus Imaging and Artificial Intelligence", published by Cornell University in the year 2021, DOI: 10.1016/j.survophthal.2022.08.005.
- [2] P.M. Siva Raja, S.L. Jothilakshmi, "Deep Learning Algorithms and Glaucoma Detection: A Review", International Research Journal of Engineering and Technology (IRJET) Volume 8, Issue 02 with Date of publication 02 Feb 2021, e-ISSN: 2395-0056, DOI: 10.1007/s42979-023-01734-z.
- [3] Pooja Sharma, Pamela A Sample, Linda M Zangwill, Joel S Schuman, "Diagnostic tools for glaucoma detection and management", National Library of Medicine Volume 53, 1st November 2018, DOI: 10.1016/j.survophthal.2008.08.003.
- [4] Amed Mvoulana, Rostom Kachouri, Mohamed Akil, "Fully automated method for glaucoma screening using robust optic nerve head detection and unsupervised segmentation-based cup-to-disc ratio computation in retinal fundus images", Science Direct, Volume 77 with Date of publication October 2019, DOI: 10.1016/j.compmedimag.2019.101643.
- [5] Abdullah Sarhan, Jon Rokne, Reda Alhaji, "Glaucoma detection using image processing techniques: A literature review", Science Direct with Date of Publication December 2019, DOI: 2019.101657.



- [6] Mahura Alessandro A. Jammal, Atalie C. Thompson, Eduardo B. Mariotoni, "Human Versus Machine: Comparing a Deep Learning Algorithm to Human Grading for Detecting Glaucoma on Fundus Photographs", American Journal of Ophthalmology with Date of Publication March 2020, DOI: 10.1016/j.ajo.2019.11.006.
- [7] M. U. Akram and Hina raja, "Detection of Glaucoma Using Cup to Disc Ratio from Spectral Domain Optical Coherence Tomography Images," in IEEE Access, Institute of Electrical and Electronics Engineers, pp. 4560-4576, 2018.
- [8] U. Raghavendra et al, "Deep convolutional neural network for accurate diagnosis of glaucoma using digital fundus images", Information Sciences, vol 441, May 2018.
- [9] Jamil Ahmad, et al., "Glaucoma detection through optic disc and cup segmentation using K-mean clustering," International Conference on Computing, Electronic and Electrical Engineering (ICE Cube), Quetta, 2016, pp. 143-147.
- [10] M. Naveed and A. Ramzan, "Clinical and technical perspective of glaucoma detection using OCT and fundus images: A review," 1st International Conference on Next Generation Computing Applications (NextComp), Mauritius, 2017, pp. 157-162.
- [11] X. Chen and Y. Xu, "Glaucoma detection based on deep convolutional neural network," 37th Annual International Conference of the IEEE Engineering in Medicine and Biology Society (EMBC), Milan, 2015, pp. 715-718.
- [12] S. Roychowdhury and D. D. Koozekanani, "Optic Disc Boundary and Vessel Origin Segmentation of Fundus Images," in IEEE Journal of Biomedical and Health Informatics, 2016, pp. 1562- 1574.
- [13] A.K Nandi and S. Sekhar, "Automated localisation of optic disk and fovea in retinal fundus images," 16th European Signal Processing Conference, Lausanne, 2008, pp. 1-5.
- [14] Yashothara S and Atheesan S., "Automatic glaucoma detection by using funduscopic images," International Conference on Wireless Communications, Signal Processing and Networking (WiSPNET), Chennai, 2016, pp. 813-817.
- [15] M. Malathi, et al, "Optic Disc and Optic Cup Segmentation for glaucoma classification," International Journal of Advanced Research in Computer Science and Technology IJARCSST, 2014.
- [16] W. Kongprawehnon, et al, "Image Processing Techniques for Glaucoma Detection Using the Cup to Disc Ratio", Thammasat International Journal of Science and Technology, 2013.
- [17] S. Chandrika, et al, "Analysis of CDR Detection for Glaucoma Diagnosis," International Journal of Engineering Research and Application ISSN, 2013.
- [18] Sandra Morales, et al, "CNNs for Automatic Glaucoma Assessment Using Fundus Images", BioMed Eng OnLine, 2019.